Interannual Variability of the Madden–Julian Oscillations in Indian Summer Monsoon Rainfall

S. V. SINGH, R. H. KRIPALANI, AND D. R. SIKKA

Indian Institute of Tropical Meteorology, Pune, India

(Manuscript received 7 January 1991, in final form 2 December 1991)

ABSTRACT

The Madden–Julian oscillations are quite prominent over the Indian monsoon region and they are related with the large-scale active-break phases of the monsoon. These oscillations, however, show considerable interannual variability in period and intensity. In this study interannual variability of these oscillations has been studied by using daily rainfall data of 365 stations for 80 years (1901–80). It is found that the intensity of these oscillations is not related with the overall performance of the monsoon and the El Niño–Southern Oscillation phenomenon.

1. Introduction

The rainfall distribution over India, even during the peak of the monsoon season, varies considerably from day to day. There are days when almost the whole country receives copious rainfall contrasted against the days when only little rain falls at a few stations. Such rainy or nonrainy situations can last for several consecutive days. Thus, over the major parts of the country, the rain occurs in spells under the influence of favorable circulation conditions. This intermittent behavior of rainfall is associated with a hierarchy of quasi periods, namely, 3–6 days, 10–20 days (Krishnamurti and Ardunay 1980), and 30–60 days (Sikka and Gadgil 1980). The latter two periods have been related with planetary-scale waves. Although the westward-moving waves, with a period in the range of 10 to 20 days, have been related by some authors to the active and break cycles (e.g., Krishnamurti and Ardunay 1980; Nagar and Singh 1991), the oscillations with a 30–60-day period are now more commonly linked with the active-break cycle of the monsoon over India (e.g., Yasunari 1981). These 30–60-day period oscillations [henceforth to be referred to as the Madden–Julian oscillations (MJOs) after Madden and Julian (1971)] are associated with the globally eastward-moving wavenumber 1 and 2 in the tropics. Over monsoon regions, particularly over India, they are characterized by poleward movement of weather anomalies including rainfall (Singh and Kripalani 1985, henceforth as SK; Hartmann and Michelsen 1989). The MJOs, however, show considerable intraseasonal and interannual variability (Mehta and Krishnamurti 1988).

In this paper we study the interannual variability of the MJOs and their evolutionary characteristics by using 80 years of rainfall data over India. In section 2 we describe the rainfall data used, and in section 3 the spatial distribution of the intensity of the MJOs. Section 4 deals with the interannual variability of the intensity of MJOs and its relationship with the total seasonal rainfall and the phases of the El Niño–Southern Oscillation (ENSO). The interannual variability of the northward progression of the rainfall anomalies characteristic of the MJOs is also studied in the same section. Important conclusions of the study are discussed in section 5.

2. Data

The daily rainfall data of 365 stations uniformly spread over the country are obtained for a period of 80 years (1901–80) from the India Meteorological Department. A few missing values are filled by linear interpolation. From these station data the spatial averages have been prepared for 52 2.5° lat/long blocks covering the contiguous country (see Fig. 1). Because of the geographical shape and orographic character of west coast rainfall, the areas considered for averaging along the west coast are in the form of strips. The density of rainfall stations is about one station per 1° lat/long area, and there are about seven stations for each block.

3. Spatial variation of intensity

For studying the intensity of the MJOs and its spatial variation, Butterworth's bandpass recursive filter (Murakami 1979), with half-power points at 30 and 60

Corresponding author address: Dr. S. V. Singh, Indian Institute of Tropical Meteorology, Dr. Homi Bhabha Marg, Pashan, Pune, 411 008, India.

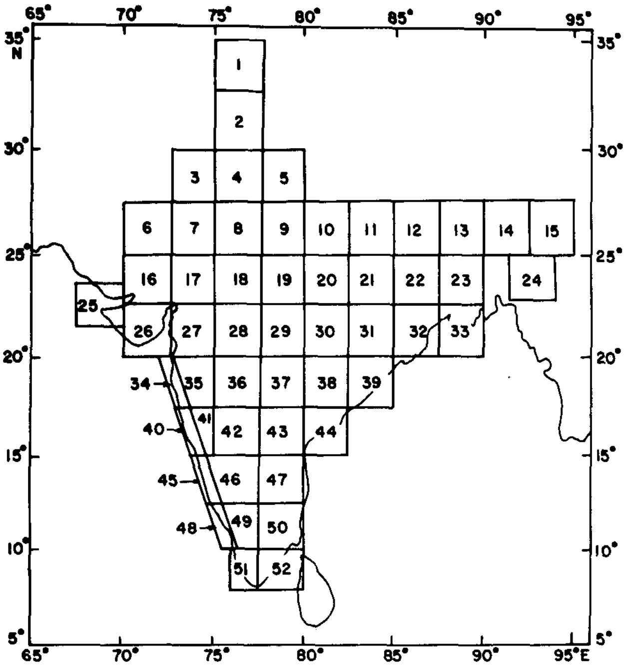

FIG. 1. Map showing the location of the 52 blocks over the Indian region.

days, is applied to the rainfall time series. This filter has the advantage of retaining nearly the full length of the time series and has been extensively employed for study of MJOs (Lau and Chan 1986; Murakami 1979). Before applying the filter to the rainfall time series of 122 days (1 Jun–30 Sep), the series have been doubled in their lengths by appending the dummy values equal to the mean of the time series (M. Murakami, personal communication). The percentage of the original variance retained by the filtered time series is then determined for each of the 80-year periods and the average of such 80 values computed. The spatial distribution of this average is shown in Fig. 2a. We find that the variance explained is highest ($\sim$10%) over the west-central parts lying between 12.5° and 22.5°N lat and west of 77.5°E long. These results are consistent with those of Lau and Chan (1986) for outgoing longwave radiation (OLR), who found that about 15% of the variance of daily OLR is explained by the 40–60-day period oscillations over this region. The average variance contained in the 30–60-day period range for the 5-day rainfall time series is also shown in Fig. 2d. As expected, the variance for the 5-day time series is nearly double ($\sim$18%) of that for the daily time series.

Both the rainfall and OLR fields show higher average intensity in the 30–60-day period range over west-central India. This results in a high correlation between these two fields over this region, in this particular frequency band, and comparatively poor relationship over other parts of the country (Kripalani et al. 1991). Since OLR is a better proxy of rainfall associated with deep convection, it may imply that the MJOs are associated with deeper convective activity over this region.

4. Interannual variability

The percentage of the variance explained by the MJOs in the individual years shows considerable variation, about half to double of what is presented in Fig. 2a. One example for a weak MJO year (1920) and a strong MJO year (1939) is presented in Fig. 2b and 2c, respectively. During 1920 (1939) the variance explained by the MJOs is about 5% (20%) over the area where the average value is 10%. For further analysis of the interannual variability of the period and intensity in the following, we consider the rainfall time series averaged over the area lying between 20°–22.5°N and 72.5°–80°E (block 27–29 in Fig. 1). This area [henceforth to be referred to as west-central India (WCI)] shows high spatial coherence and intensity of the MJOs.

a. Interannual variability of period

At first we apply the maximum entropy spectral analysis (MESA) to all time series. The MESA is an efficient method for identifying long periods from short time series. The theoretical foundation and the advantages of this method of spectrum analysis can be found

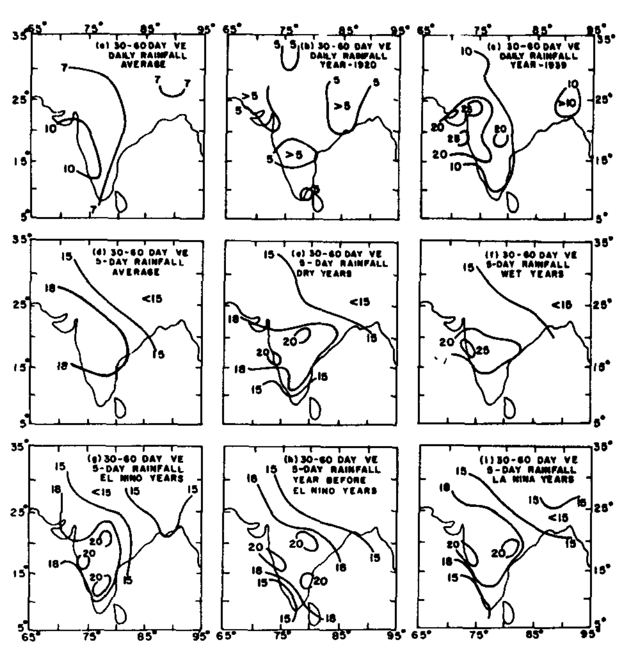

FIG. 2. Percentage of the variation explained by the 30–60-day band. (a) Average based on 80 years for daily rainfall, (b) for the year 1920, (c) for the year 1939, (d) average based on 80 years for 5-day rainfall, (e) average of 17 dry monsoon years, (f) average of 15 wet monsoon years, (g) average of 21 warm episode years, (h) average of 21 years before warm episode years; (i) average based on 25 cold episode years.

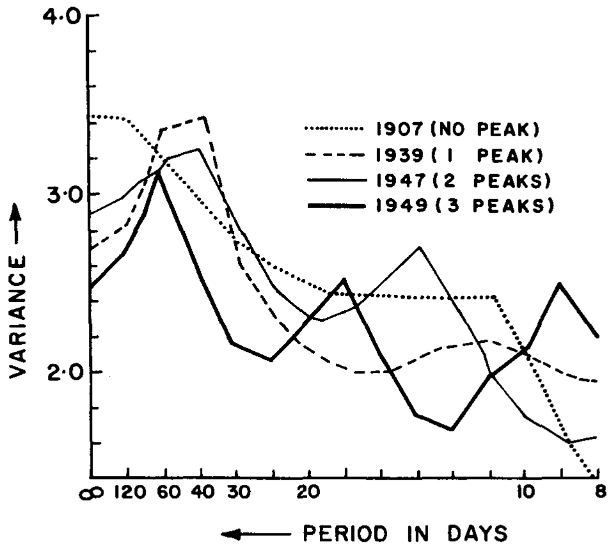

FIG. 3. Examples of the number of peaks in the spectra of the daily rainfall over central India. · · · · · No peak for the year 1907; – – – 1 peak for the year 1939; —— 2 peaks for the year 1947; —— 3 peaks for the year 1949.

in Ulrych and Bishop (1975). The length of the time series of WCI rainfall is 122 days (1 Jun–30 Sep), and a lag of 25 days ($\sim N/5$) is found suitable for computation of spectra after several experiments. We have plotted all 80 spectra corresponding to each of the 80 years for the period range 9–120 days, omitting shorter periods. The spectra are found to differ considerably from year to year. The number of peaks in the period range examined vary from 0 to 3. One example of each type of spectra is shown in Fig. 3. A subjective assessment of the number of peaks reveals that there are 0, 1, 2, and 3 peaks, respectively, in 12, 36, 22, and 10 years. During 36 years having 1 peak, 22 showed peaks in the range of 30–60 days, and 14 in the range of 8–30 days. During the 22 years having 2 peaks, the most dominant peak always lays in the 30–60-day period range. In 8 of the 10 years having 3 peaks, the highest peak had a period of 60 days and the second highest peak was near a 20-day period.

Some authors recently have pointed out from the analysis of limited data that the interannual variability of the MJOs is linked with the overall performance of the monsoon (e.g., Chowdhury et al. 1988). For examining this hypothesis we have prepared the scatterplot between the exact period of the peaks in the 30–60-day range and the standardized all–India monsoon rainfall (SAIMR) taken from Parthasarathy et al. (1987). This scatterplot (Fig. 4a) does not suggest any linear relationship between the periods of MJO and the overall performance of the monsoon.

The above description of the peaks is rather subjective, but it suggests that the occurrence of spectral peaks in the 30–60-day period range over WCI is rather a common feature observed on at least 50% of the occasions. We are unable to quantify and test the significance of these peaks because of the lack of such standard techniques in application of MESA. Other techniques of spectral analysis could be employed for which the standard procedures of significance testing exist, but these techniques have rather poor resolution.

b. *Interannual variability of intensity*

We have noted above that the variance due to MJOs can vary from half to double of their average magni-

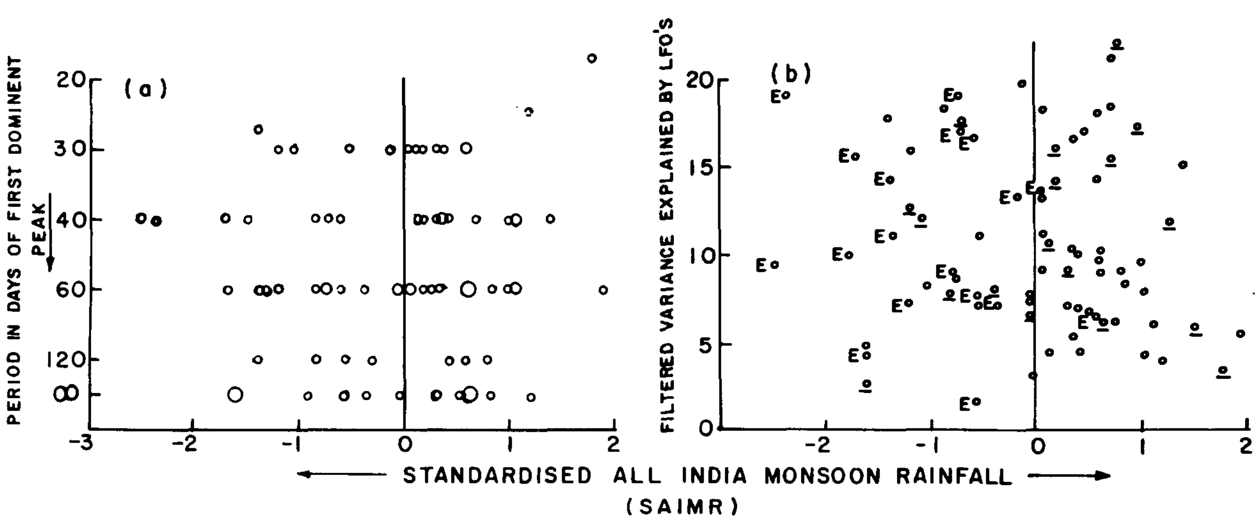

FIG. 4. Scatterplot between (a) exact period of the peaks in the 30–60-day band and the SAIMR. (b) Percentage of the variance explained by the MJOs and SAIMR. Bigger circles in (a) denote more than one value at that point. The *E* in (b) represents El Niño and a dash (–) below the point represents a La Niña year.

tude. For getting a better quantitative idea about the range of variability, we have set out in Table 1 the variance explained by the 10 strongest and weakest MJO years. The choice of 10 years is rather arbitrary. The mean variance explained by these sets of 10 years is 19.2% and 3.7%, respectively. The maximum and minimum values for individual years are 21.9% and 1.7%, respectively. The SAIMR is also given in the table for enabling examination of the MJOs intensity with respect to total seasonal rainfall. We find that the strong MJOs can be associated with negative as well as positive departure of seasonal rainfall. Even though the negative rainfall departures have higher magnitude in this set of 10 years, a relationship between the intensity of MJOs and the seasonal rainfall is not apparent. This view is supported more clearly when the years of weak MJOs are examined. Now we find that equally strong positive and negative anomalies of seasonal rainfall can occur in association with weak MJO. To further examine the relationship, a scatterplot between the MJO intensity and the SAIMR for all 80 years is prepared (Fig. 4b). This plot, again like the period (Fig. 4a), does not show any linear relationship between MJO intensity and the seasonal rainfall.

For examining the changes in intensity of MJO over the whole country, with respect to monsoon rainfall, we utilize the bandpass-filtered series of 5-day rainfall. Composite charts of variance explained for the ranked 17 dry and 15 wet years are shown in Figs. 2e and 2f. A departure of ±8% from normal has been considered for defining these wet/dry years. We find that there is practically no difference between the average variance explained by the MJOs for these two sets of years. The relationship between the MJO and the various phases of ENSO is also similarly examined by preparing composite charts for 21 warm and cold Pacific sea surface temperature years (Figs. 2g and 2i). Also, for checking

TABLE 1. Percentage of the variance retained by the 30–60-day bandpass filter over WCI for the 10 strongest and 10 weakest MJOs. VE-variance explained; SAIMR-Standardized all India Monsoon rainfall.

	Strong MJOs			Weak MJOs		
	Year	VE	SAIMR	Year	VE	SAIMR
1.	1964	21.9	0.82	1925	1.7	−0.59
2.	1934	21.4	0.73	1901	2.6	−1.60
3.	1960	19.8	−0.16	1927	2.9	−0.03
4.	1972	19.0	−2.39	1971	3.5	1.82
5.	1939	18.9	−0.76	1942	3.9	1.27
6.	1973	18.7	0.72	1905	4.1	−1.64
7.	1915	18.3	−0.86	1970	4.2	1.05
8.	1967	18.2	0.09	1943	4.4	0.17
9.	1946	17.9	0.59	1920	4.8	−1.62
10.	1966	17.8	−1.40	1948	5.3	0.24
	Mean	19.2		Mean	3.7	

the hypothesis of Lau and Chan (1986) that the MJOs are active before the onset of warm episodes (El Niño events), we have prepared another composite chart for the years preceding the El Niño years (Fig. 2j). This chart, again, does not differ from those presented in Figs. 2g and 2i in any recognizable way, suggesting absence of relationship between the MJOs over the Indian region and the phases of the ENSO.

c. Progression characteristics

For studying the interannual variability of the northward progressions we have constructed the Hovmöller diagrams for all 80 years. It may be noted that a few Hovmöller diagrams showing northward progressions of rainfall anomalies across central longitudes of India were presented in SK by using unfiltered data. Considerable interannual and intraseasonal variabilities in the propagation characteristics were noted. For example, in the early part of 1969 the progression recurred at intervals of 20 days and in the latter part of the same year the progression recurred at intervals of about 40 days. The year 1972 was characterized by one progression of negative and one progression of positive anomaly in the early part of the year. During the remaining part of this year, by and large, the anomalies were of the standing or nonprogressive type affecting most parts of the country simultaneously (Fig. 4 of SK). In the present study we have prepared the latitude–time cross section for the longitudinal belt between 75° and 80°E by using 30–60-day bandpassed-filtered pentad rainfall anomalies. After an examination of these cross sections it has been found that the northward progressions of the rainfall anomalies are organized during about half of the years. A few years exhibit combination of southward and northward progressions.

Some typical examples of the Hovmöller diagrams are presented in Fig. 5. In 1906 the progressions are well organized and occur at nearly uniform intervals. However, the intensity is not uniform along the course of the progressions. It is maximum for the latitude belt lying between 20.0°–22.5°N. The intensity of the progressions decreases northward to increase again near 27°N lat. These two latitude positions correspond to the quasi-stationary positions of the monsoon trough at 700-hPa level during the active and break monsoon conditions, respectively. Many times the region south of 20°N appears to have been simultaneously influenced by the progressions. On such occasions the starting latitude of the progressions cannot be precisely determined. This near-simultaneous influence of latitude belts south of 20°N has also been noted by Cadet and Daniel (1988) and Hartmann and Michelsen (1989). As noted above, all years do not show such organized progressions throughout the season, as observed during the First GARP (Global Atmospheric Research Pro-

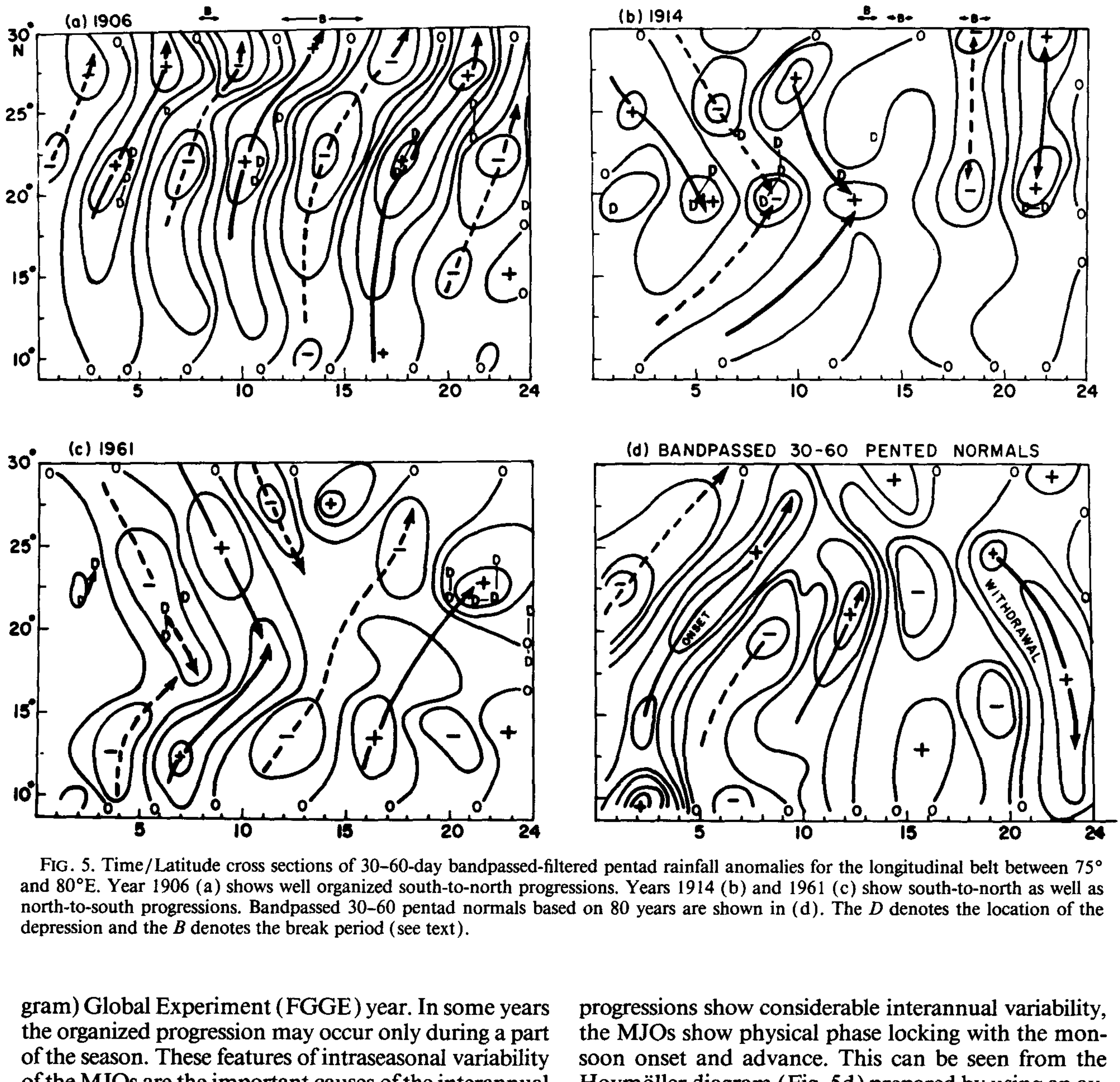

FIG. 5. Time/Latitude cross sections of 30–60-day bandpassed-filtered pentad rainfall anomalies for the longitudinal belt between 75° and 80°E. Year 1906 (a) shows well organized south-to-north progressions. Years 1914 (b) and 1961 (c) show south-to-north as well as north-to-south progressions. Bandpassed 30–60 pentad normals based on 80 years are shown in (d). The *D* denotes the location of the depression and the *B* denotes the break period (see text).

gram) Global Experiment (FGGE) year. In some years the organized progression may occur only during a part of the season. These features of intraseasonal variability of the MJOs are the important causes of the interannual variability of their intensity. During part of a few other years, the rainfall anomalies progress from south to north and north to south, simultaneously, to meet at some intermediate position generally between 20°N and 22.5°N lat. The remaining parts of such years may be characterized by stationary fluctuations (example 1914) or south to north progressions (example 1961). These are the typical examples of midlatitude tropical interaction during monsoon season. Such simultaneous progressions from south and north have been noted in the west Pacific by Murakami (1984). An example of southward progression of anomalies in the recent year 1984 has also been discussed by Krishnamurti et al. (1989). Even though the period and intensity of the progressions show considerable interannual variability, the MJOs show physical phase locking with the monsoon onset and advance. This can be seen from the Hovmöller diagram (Fig. 5d) prepared by using an average of 80 bandpass-filtered time series. A weak progression of one negative and one positive anomaly after the onset and the southward progression of the anomalies related with the withdrawal can also be observed in this diagram.

We have noted that the northward progression of rainfall anomalies is not always prevalent during the monsoon season. In order to find out the proportion of time during which such progressions are prevalent, we have counted the total number of pentads involved in northward progression near 20°N lat. This showed that about 70% of the pentads are involved in northward progression of anomalies. However, the period and speed of progression of rainfall anomalies differed from episode to episode. The median speed of progression is 0.5° lat day^{-1}. During the widely studied year 1979 the speed of progression was about 0.75° lat day^{-1} (Krishnamurti and Subramanyam 1982; Lorenc 1984).

5. Conclusions

Existence of the southward-to-northward progression of the summer rainfall anomalies over India related with the MJOs had been noted by the authors earlier. Here we have studied the spatial and temporal (interannual) variability of these oscillations in the monsoon rainfall. From this study the following two conclusions are drawn:

(i) The Madden–Julian oscillations are strongest over west-central India where they explain 10%(20%) of the variance of the daily (5-day) rainfall. This result is consistent with those of Lau and Chan (1988) and others for outgoing longwave radiation data.

(ii) These oscillations show considerable interannual variability in intensity ranging from about half to double the average value. They are not well organized in every year, and only about 40% of the years exhibit organized oscillations. This variability of MJOs does not show any linear relationship with total seasonal monsoon rainfall or the phases of the El Niño–Southern Oscillation phenomenon. These results agree with those of Gray (1988) but contradict the findings of other authors who have noted some linkage between MJOs and the ENSO (e.g., Lau and Chan 1988) and seasonal rainfall (Chowdhury et al. 1988). One possible reason for this contradiction is that these authors have used only limited years of data in their study. Here we have used a sufficiently long period (80 years) of data. From our results we are tempted to conclude that the MJOs representing a type of intraseasonal variability, though of longest period, should be considered as climate noise as far as interannual variability is considered (Madden 1976). If there exists any relationship between the MJO intensity and ENSO, it is very subtle to be detected by the rainfall data over the Indian region or the method of analysis followed. Absence of empirical relationship does not deny the triggering of the ENSO process by the MJOs in individual cases. It remains to be examined if the interannual variability of the MJOs in any other weather element shows definite relationship with ENSO events or if there is any other method that can bring out such a relationship empirically.

Acknowledgments. The authors are thankful to Dr. S. S. Singh, head of the Forecasting Research Division, for encouragement and interest in this study. We are also thankful to Dr. B. Parthasarathy and Mr. D. K. Paul for going through the manuscript, to Dr. M. Murakami for explaining some aspects of the bandpass filter used, and to Bob Livezey for painstaking editing work. The station rainfall data were obtained from India Meteorological Department.

REFERENCES

Cadet, D. L., and P. Daniel, 1988: Long-range forecast of the break and active summer monsoons. *Tellus,* **40A,** 133–150.

Chowdhury, A., R. K. Mukhopadhyay, and K. C. Sinha Ray, 1988: Low frequency oscillations in summer monsoon rainfall over India. *Mausam,* **39,** 375–382.

Gray, B. M., 1988: Seasonal frequency variations in the 40–50 day oscillations. *J. Climatol.,* **8,** 511–519.

Hartmann, D. L., and M. L. Michelsen, 1989: Intraseasonal periodicities in Indian rainfall. *J. Atmos. Sci.,* **46,** 2838–2862.

Kripalani, R. H., S. V. Singh, and P. A. Arkin, 1991: Large-scale features of rainfall and outgoing longwave radiation over Indian and adjoining regions. *Contrib. Atmos. Phys.,* **64,** 159–168.

Krishnamurti, T. N., and P. Ardunay, 1980: The 10 to 20 day westward propagating mode and "breaks" in the monsoon. *Tellus,* **32,** 15–26.

——, and D. Subrahmanyam, 1982: The 30–50 day mode at 850 mb during MONEX. *J. Atmos. Sci.,* **39,** 2088–2095.

——, M. Subramaniam, D. K. Oosterhof, and G. Daughenbaugh, 1989: Predictability of low frequency modes. FSU Rep. No. 89-9, Dept. of Meteorology, Florida State University, Tallahassee, FL, 28 pp.

Lau, K. M., and P. H. Chan, 1986: The 40–50 day oscillation and the El Niño/Southern Oscillation: A new perspective. *Bull. Amer. Meteor. Soc.,* **67,** 533–534.

——, and ——, 1988: Intraseasonal and interannual variations of tropical convection: A possible link between the 40–50 day oscillation and ENSO. *J. Atmos. Sci.,* **45,** 506–521.

Lorenc, A. C., 1984: The evolution of planetary scale 200 mb divergent flow during the FGGE year. *Quart. J. Roy. Meteor. Soc.,* **110,** 427–442.

Madden, R. A., 1976: Estimates of the natural variability of time averaged sea-level pressure. *Mon. Wea. Rev.,* **104,** 942–952.

——, and P. R. Julian, 1971: Detection of a 40–50 day oscillation in the zonal wind in the tropical Pacific. *J. Atmos. Sci.,* **28,** 702–708.

Mehta, A. V., and T. N. Krishnamurti, 1988: Inter-annual variability of 30 to 50 day wave motions. *J. Meteor. Soc. Japan,* **66,** 535–548.

Murakami, M., 1979: Recursion technique for Band-pass filter. *Mon. Wea. Rev.,* **107,** 1011–1012.

——, 1984: Analysis of deep convective activity over the western Pacific and Southeast Asia. Part II: Seasonal and intraseasonal variations during northern summer. *J. Meteor. Soc. Japan,* **62,** 88–108.

Nagar, S. G., and S. V. Singh, 1991: Variations of surface pressure over India during southwest monsoon. *Theor. Appl. Climatol.,* **44,** 95–112.

Parthasarathy, B., N. A. Sontakke, A. A. Munot, and D. R. Kothawale, 1987: Droughts/floods in the summer monsoon season over different meteorological subdivisions of India for the period 1871–1984. *J. Climatol.,* **7,** 57–70.

Sikka, D. R., and S. Gadgil, 1980: On the maximum cloud zone and the ITCZ over Indian longitudes during the southwest monsoon. *Mon. Wea. Rev.,* **108,** 1840–1853.

Singh, S. V., and R. H. Kripalani, 1985: The south to north progression of rainfall anomalies across India during the summer monsoon season. *Pure Appl. Geophys.,* **123,** 624–637.

Ulrych, T. J., and T. N. Bishop, 1975: Maximum entropy spectral analysis and autoregressive decomposition. *Rev. Geophys. Space Phys.,* **18,** 183–200.

Yasunari, T., 1981: Structure of an Indian summer monsoon system with around 40-day period. *J. Meteor. Soc. Japan,* **59,** 336–354.